ACS APPLIED MATERIALS & INTERFACES

Research Article

www.acsami.org

Efficient Solvent-Assisted Post-Treatment for Molecular Rearrangement of Sprayed Polymer Field-Effect Transistors

Hye-Yun Park,[†] Hoichang Yang,[‡] Si-Kyung Choi,[†] and Sung-Yeon Jang*[,§]

[†]Department of Material Science and Engineering, Korea Advanced Institute of Science and Technology, Daejeon, 305-701, Korea

[‡]Department of Advanced Fiber Engineering, Inha University, Incheon 402-751, Korea

[§]Department of Chemistry, Kookmin University, 861-1 Jeongneung-Dong, Seongbuk-Gu, Seoul, 136-702, Korea

Supporting Information

ABSTRACT: Polymer-based field-effect transistors are fabricated using the gas-assisted spray technique, and their performance is considerably improved when a solvent-assisted post-treatment method, solvent sprayed overlayer (SSO), is used. The SSO method is a unique treatment that can facilitate chain packing to increase crystallinity within the sprayed polymer layers, which inherently have a kinetically trapped amorphous chain morphology with lack of crystallinity due to rapid solvent evaporation. The device performance was drastically improved after SSO relative to conventional post-treatment, thermal annealing (TA). This occurred because SSO can rearrange the polymer chains into a dominantly edge-on crystal orientation, which is preferential for charge transport, whereas TA increases the crystallinity without rearrangement of the crystal orientation resulting in a complex of edge-on and face-on. The development of edge-on crystal domains after SSO within the active layers was responsible for the significant improvement in performance. The SSO is a simple and effective post-treatment method that validates the use of spray process and holds promise for use in other high-throughput processes for OFETs fabrication.

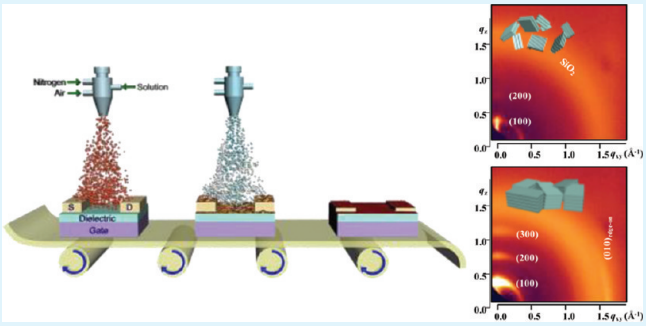

KEYWORDS: *organic thin film transistor, spray deposition, solvent assisted treatment, poly(3-hexylthiophene), molecular packing*

INTRODUCTION

Organic field-effect transistors (OFETs) have received significant attention because of the potential use in flexible and/or disposable portable electronic devices.[1−3] Although the performance of solution-processable OFETs has improved through the design of organic materials,[4,5] the development of advanced processing strategies for low-cost, large-area, and continuous manufacturing methods are still obstacles preventing commercialization.[4,6−16] There has recently been several reports on OFETs using various solution-processing techniques, such as dip-coating,[17,18] spin-coating,[11] inkjet printing,[12,13] spray coating,[14] and screen printing.[10,15,16] Among them, the spray-coating method has emerged as a potential approach to overcome the practical processing issues for organic materials (especially polymers) because it is high-throughput, easily scalable for large-area deposition on various substrates, and can be readily adapted to a roll-to-roll (R2R) process. Polymer-based organic electronic devices such as photovoltaics, photodiodes, and ligh-emitting diodes using spray technique have received tremendous attention.[19−23]

In OFETs, the charge transport in an active layer is largely influenced by molecular ordering/packing and density of grain boundaries.[9,24−28] Thus, the formation of active films that possess a preferential molecular ordering and packing is crucial to achieve high device performance.[9,26,29,30] In the solution process, molecular ordering is often achieved by self-assembly during solvent drying. Therefore, the detailed processing conditions for active film formation (deposition) can influence the resulting molecular order. Extensive efforts to control molecular ordering of the organic active layers have been made by reducing the solvent evaporation rate during film formation using high boiling point solvent/additives,[25,29,31,32] or under saturated solvent vapors.[29] This approach was shown to produce thermodynamically determined crystal structures with diminished grain boundaries. Controlling the surface energy at the dielectric/active layers interface by surface treatment such as molecular self-assembled monolayers (SAMs) could also facilitate molecular ordering.[9,33−35] Reassembly of the polymer chains within the predeposited active layers by post-treatments has also been attempted. Annealing above the melting temperature (T_m) of polymers could alter the molecular orientation toward a preferential direction.[30,33] Soaking the films under solvent vapors could also reflow the polymer chains and increase the crystallinity.[36]

Received: September 19, 2011
Accepted: December 10, 2011
Published: December 11, 2011

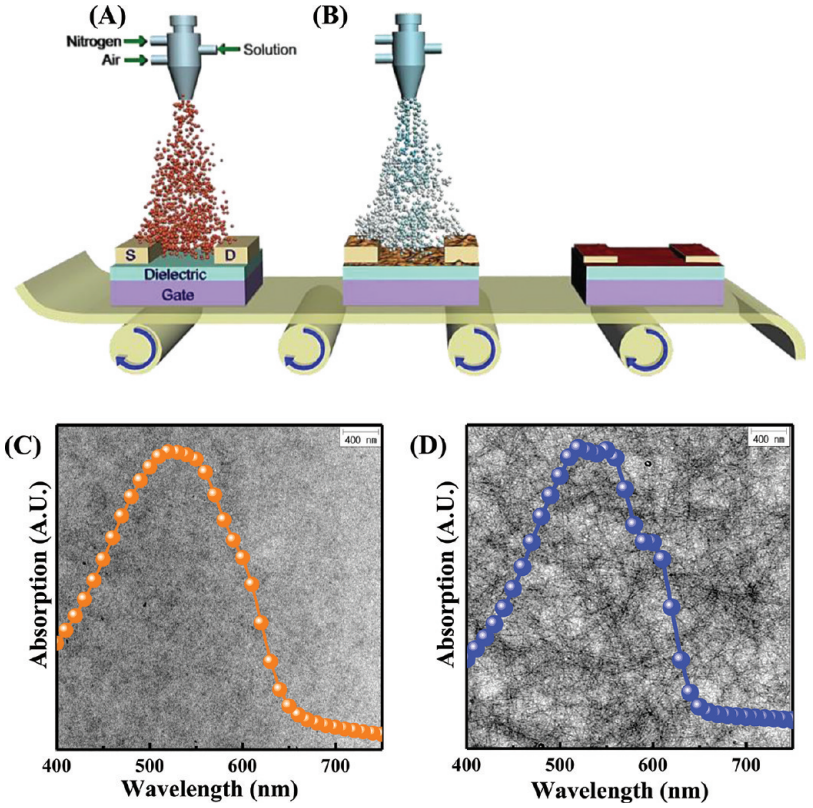

Figure 1. (A, B) Schematic description of OFET fabrication using the g-spray method and (C, D) crystallinity characterization results; (A) P3HT active layer preparation using the g-spray method, (B) SSO post-treatment, (C) UV−vis absorption spectra and bright-field TEM image (background) of the as-sprayed P3HT active films, (D) UV−vis absorption spectra and bright-field TEM image (background) of the SSO-treated P3HT active films. The P3HT film thickness was ∼80 nm. The spray time for SSO was 4 s under an air atmosphere.

However, these post-treatment routes either require unrealistically high temperature (>240 °C)[30,33] or is plagued by the high chance of substantial film dewetting.[36] Furthermore, efforts to optimize the internal molecular ordering/packing of active layers in parallel with the development of practical processing techniques have been elusive. Development of external post-treatment methods that can control the self-organizing molecular ordering regardless of the film deposition techniques will facilitate the commercialization of OTFTs.

In the case of spray deposition methods, the films are formed by the continuous deposition of droplets that are atomized by the application of gas flow or electric field. To form a continuous film without dewetting, the removal of residual solvents should be fast enough.[19,20,37−39] This unique requirement often limits the realization of sufficient molecular ordering in large-area deposition because the rapid solvent evaporation produces polymer chains that have a kinetically trapped random conformation. Methods to overcome these shortcomings have been developed in which the polymer solutions in mixed solvents are sprayed onto heated substrates.[14,37] However, the development of spray adaptable and more practical external control methods, which can optimize the internal molecular ordering/packing of the as-sprayed films, may be a more efficient strategy in regards to capitalizing the advantages of the spray technique for OFET fabrication.

In this study, high-performance OFETs were fabricated by a gas-assisted spray (g-spray) deposition method using poly(3-hexylthiophene) (P3HT), a prototype material for polymer based OFETs, as an active material. The chain orientation and packing within the active layer, which is the most crucial factor dictating the performance of OFETs, could effectively be rearranged by a novel solvent assisted post-treatment method, solvent spray overlayer (SSO). In SSO, the as-sprayed P3HT films were treated with a brief solvent spray for a short time (<5 s.) and dried for a period of a few minutes at room temperature. After SSO, the device performance was dramatically enhanced as a result of preferential molecular rearrangement. The effect of the SSO on the molecular packing and orientation was chracterized using ultraviolet−visible (UV−vis) spectroscopy, transmission electron microscopy (TEM), and two-diensional (2D) grazing-incident X-ray diffraction (GIXRD) analysis. The effect of thermal annealing (TA), which has been shown to be an effective post-treatment method for OFETs,[7,17,18,40] on chain ordering and device performance was also compared. While there are not many practical methods for chain rearrangement, this facile SSO treatment could effectively reconstruct the P3HT into a preferential edge-on orientation within the g-sprayed polymer active layers.

EXPERIMENTAL METHODS

Preparation of Substrates. The bottom contact FETs were fabricated on highly doped n-type (100) silicon substrates containing 300 nm silicon dioxide (SiO_2) layers. Cr/Au (20 nm/200 nm) layers on the substrates were patterned by photolithography and used as the source and drain electrodes. The channel length/width (L/W) was 50 μm/1000 μm. After cleaning using a H_2SO_4/H_2O_2 solution at 80 °C for 45 min, all substrates were immersed in a 0.5 mM octadecyltrichlorosilane (OTS) solution in anhydrous toluene (Sigma-Aldruch, 99.8%) for 12 h.[35] Finally, the patterned substrates were successively sonicated in baths of chloroform, isopropanol, and

dx.doi.org/10.1021/am201274s | ACS Appl. Mater. Interfaces 2012, 4, 214−221

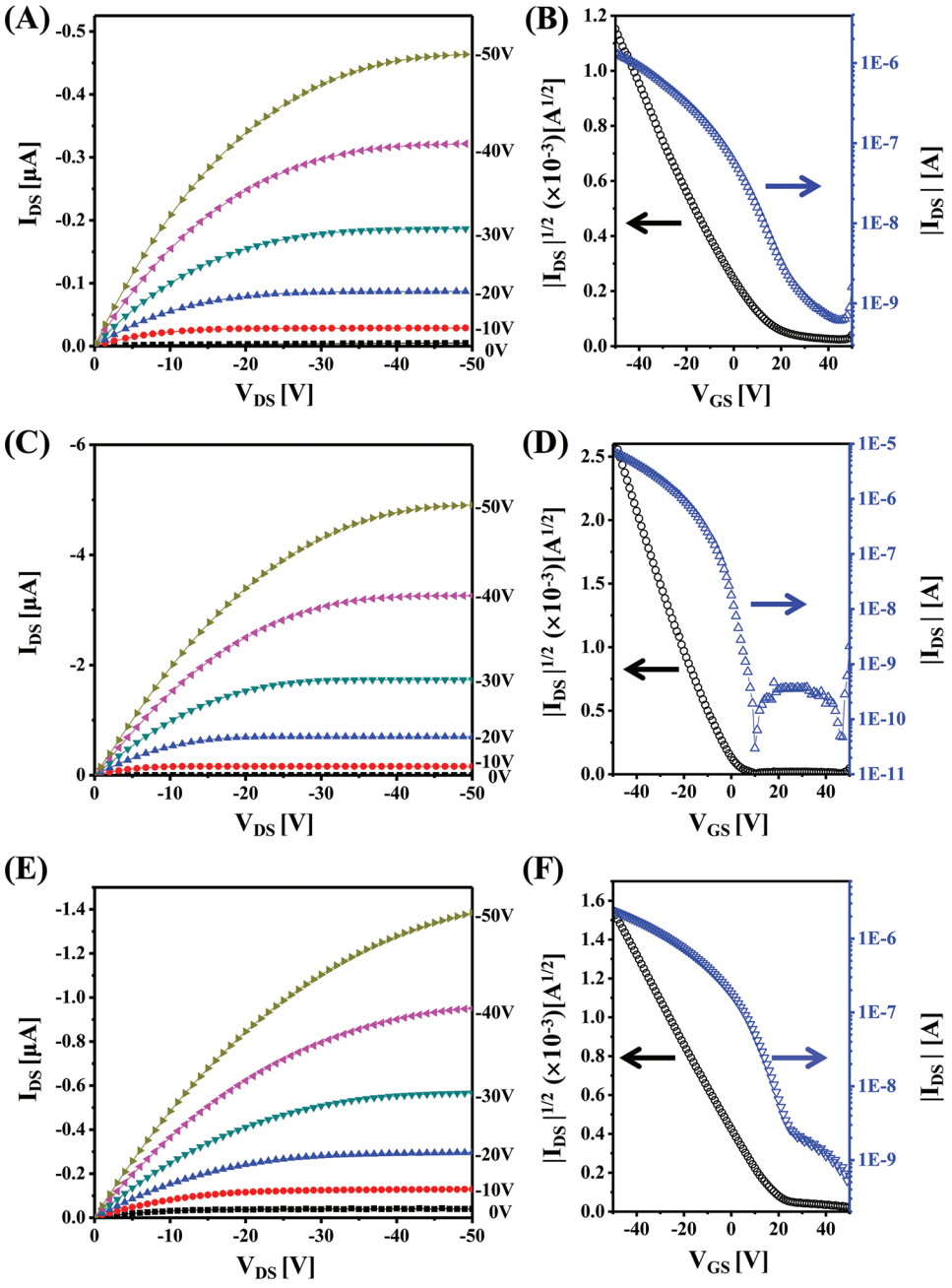

Figure 2. Current−voltage (I−V) output (V_{DS} = 0 to −50 V) and transfer characteristic curves (V_{GS} = +50 to −50 V) of the sprayed OFETs; (A, B) as-sprayed device, (C, D) SSO-treated device, (E, F) TA treated device. The spray time for SSO was 4 s under an air atmosphere. TA was performed at 135 °C for 30 min under N_2.

deionized water and dried for 1 h in a vacuum oven (~1 × 10^{-3} Torr.) at 80 °C.

Deposition of Active Layers by g-spray Method. Two mg of regioregular P3HT (REIKE Metals, RR ≈ 95%, M_n =50 000 g mol^{-1}) was disolved in 1 mL of chlorobenzene (CB, Sigma-Aldrich) and stirred for >4 h. In order to spray the P3HT solution, the substrates were placed on the sample holder, which was kept ~25 cm away from the spray nozzle tip. The P3HT solution was atomized onto a substrate at a rate of 0.18 mL min^{-1} by applying N_2 gas at a pressure of 0.4 Kg f cm^{-2} using a conventional gas-spray gun.

Post-Treatments (SSO and TA). For the SSO treatment, the as-sprayed P3HT active layers were subsequently exposed to an additional spray of dichlorobenzene (DCB), which was atomized at a rate of ~1.5 mL min^{-1} (at the N_2 gas pressure of 0.2 Kg f cm^{-2}), ~2 s. The distance between the substrates and the spray nozzle was ~30 cm. After spraying the P3HT films with DCB, the wet films were left under ambient air conditions for <5 min. TA was carried out in a drybox under a nitrogen atmosphere at 135 °C for 30 min.

Device Characterization. The charge transport characteristics of the g-sprayed FET devices were measured in the saturation regime (drain volatage V_D = −50 V) using a semiconductor parameter analyzer (Agilent B1500A). All samples were completely dried in a vacuum oven at 80 °C for 3 h before characterization and measured under ambient air condtions. The value of the field effect mobility for each device was caculated from the transfer curves acquired at a gate-voltage range of +50 to −50 V with 1 V steps using the following equation:

$$I_{Dsat} = \left(\frac{WC_{OX}}{2L}\right)\mu_{sat}(V_{GS} - V_T)^2$$

dx.doi.org/10.1021/am201274s | ACS Appl. Mater. Interfaces 2012, 4, 214−221

Where C_{OX} is the oxide capacitance per unit surface, L is channel length, W is channel width, and V_T is the threshold voltage.

Chracterization of Active Films. A surface profilometer (Alpha-Step IQ Profilers) was used to measure the film thicknesses. In order to examine the evolution of P3HT crystallinity, samples were evaluated using transmission electron micruoscopy (TEM) and ultraviolet−visible spectroscopy (UV−vis). For TEM analysis, a JEM 3010 JEOL at 300 kV was used. The spayed P3HT active films (50−80 nm thick) were floated using hydrofluoric acid and transferred to 200-mesh copper grids. UV−vis absorption spectra of the active films were obtained using a Lambda 35 spectrophotometer.The P3HT molecular ordering was verified by Synchrotron-based grazing-incident X-ray diffraction (GIXRD) using the X9 beamline at the national Synchrotron Light Source (NSLS) in the Brookhaven National Laboratory. Samples were mounted on a three-axis goniometer and the scattered intensities were recorded using a 2D MarCCD. 2D GIXRD patterns were monitored in the range of $0 < q_z < 1.97$ Å^{-1} and $0 < q_{xy} < 2.05$ Å^{-1}. In this case, the incident beam angle was >0.18° to increase the scattered intensities.

RESULTS AND DISCUSSION

A schematic description of the g-spray technique used to prepare our P3HT active layers and the structure of OFETs are shown in Figure 1. For active layer deposition, the P3HT solution (∼0.2 wt %) in chlorobenzene was atomized at a rate of 0.18 mlmin^{-1} by supplying N_2 gas at a pressure of 0.4 Kg f cm^{-2} through a conventional spray gun onto patterned substrates that were placed ∼25 cm away from the nozzle tip (Figure 1A). Details on the preparation of the P3HT solutions and patterned substrates are discribed in the experimental section. SSO post-treatment of the sprayed P3HT active layer was performed by spraying dichlorobenzene (DCB) for 2−5 s at a rate of ∼1.5 mL min^{-1} (Figure 1B) followed by drying under an air atmosphere over a period of ∼5 min. Spectra C and D in Figure 1 show the UV−vis absoption of g-sprayed P3HT films. UV−vis absorption analysis has been used to investigate the molecular packing of P3HT where the vibronic features near the wavelengths of 550 and 610 nm orginate from the interchain $\pi-\pi$ packing.[41,42] The as-sprayed films exhibited characteristic absorptions of P3HT without discernible vibronic features (Figure 1C). After SSO treatment, the vibronic features of the g-sprayed film were considerably more pronounced (Figure 1D), indicating the development of higher ordered crystalline P3HT. The development of the P3HT crystals upon SSO treatment was also confirmed by TEM analysis. The backgroud bright-field TEM (BF-TEM) images in Figure 1D clearly demonstrated the presence of self-assembled nanoscale P3HT fibrils (∼tens of nanometers wide), which is typical of the P3HT ordring,[31,43,44] whereas no nanofibrils were observed in the as-sprayed films (Figure 1C). These UV−vis and TEM results suggested that the fast solvent drying rate during the g-spray deposition process limited the crystallization (or molecular packing) of P3HT and enclosing kinetically trapped chain conformation. However, chain repacking in the nano-fibrillar crystals could be effectively achieved by SSO post-treatment.

Figure 2 shows the current−voltage ($I-V$) output and transfer characteristic curves of the OFETs using the g-sprayed P3HT active layers. All devices were fabricated using the bottom contact geometry and operated in accumulation mode as described in the experimental section. The devices displayed prototypical $I-V$ characteristics of P3HT based OFETs at room temperature and under ambient air conditions. The performance of devices containing the SSO treated active layers (panels C and D) was better than the as-sprayed layers (panels A and B) and these devices exhibited higher currents with good saturation behavior and conformed well to the conventional FET models in both the linear and saturated regimes. The extracted charge mobility of SSO treated device was as high as 0.02 cm^2/(V s) with a current on/off ratio of ∼1 × 10^5, while that of the as-sprayed devices was ∼0.0016 cm^2/(V s) with a current on/off ratio of ∼1 × 10^3. The mobility values were calculated from transfer curves swept in the gate-voltage range of +50 to −50 V. The turn-on voltages obtained from $|I_D|$ vs V_{GS} and threshold voltage (V_{th}), which were determined from a linear extrapolation of $|I_D|^{1/2}$ vs V_{GS}, were also lower in the devices containing the SSO treated active layers. The values from the $I-V$ characterization were summarized in Table 1. We

Table 1. Detailed Values of OFETs Performance

	V_{th} (V)	μ (cm^2 V^{-1} s^{-1})	I_{on}/I_{off}
AS	8.5 ± 5.2	0.0013 ± 0.0011	2.43 × 10^3
TA	17 ± 4.5	0.0024 ± 0.0015	7.78 × 10^3
SSO	−3.8 ± 2.2	0.0230 ± 0.013	2.41 × 10^5
SSO/TA	−5.2 ± 3.4	0.0295 ± 0.015	1.80 × 10^5

also characterized devices containing the TA treated g-sprayed active layers in order to compare the effect of two different post-treatments. In these experiments, the performance of devices containing the g-sprayed OFETs that had been subjected to post TA treatment (Figure 2E, F) was lower than devices subjected to SSO treatment as shown in Table 1. The significant difference in the performance of the devices by the two treatments (SSO and TA) was intriguing because TA is known to be a very efficient post-treatment strategy for enhancing the performance of OFETs fabricated by spin-casting or dip-coating methods through chain ordering and charge injection barrier lowering.[7,17,18,40] In order to understand the reason for the improved performance after SSO treatment, the nanoscale chain ordering within the g-sprayed P3HT active layers were further investigated.

The performance of OFETs is mainly determined by the molecular ordering in the active layers. It is known that P3HT is a semicrystalline material, where polycrystalline domains are embedded in an amorphous matrix, and the charge transport is dominated by the crystallinity, crystal orientation, and grain boundary effects.[26,28,29,45] McGehee and co-workers reported that the difference in crystal orientation rather than the difference in crystallinity was the more critical parameter affecting the charge transport properties of P3HT active layers.[9,44,46] In order to further understand the effect of SSO treatment on the chain ordering/packing, 2D-GIXRD analysis was performed. 2D-GIXRD provides detailed information on crystallinity and the crystal orientation in organic thin films.[25,29,45] Figure 3 shows the 2D-GIXRD patterns and the out-of-plane one-dimentional (1D) profiles of the g-sprayed P3HT active layers. All films had a thickness of ∼80 nm. The low degree of crystallinity and ordering of the as-sprayed active layers was revealed by the lack of apparent 2D-GIXRD patterns along both the q_z (out-of-plane) and q_{xy} (in-plane) axes (Figure 3A) which was confirmed by the absence of discernible peaks in the 1D profiles (Figure 3E). The enhancement in crystallinity upon both post-treatments (SSO and TA) of the as-sprayed P3HT films was clearly observed in the XRD patterns (Figure 3B−D). In TA treated films, both (h00) and (010) patterns were observed on the out-of-plane (q_z) axis as indicated in Figure 3B. However, in the case of SSO-treated films, the (010)

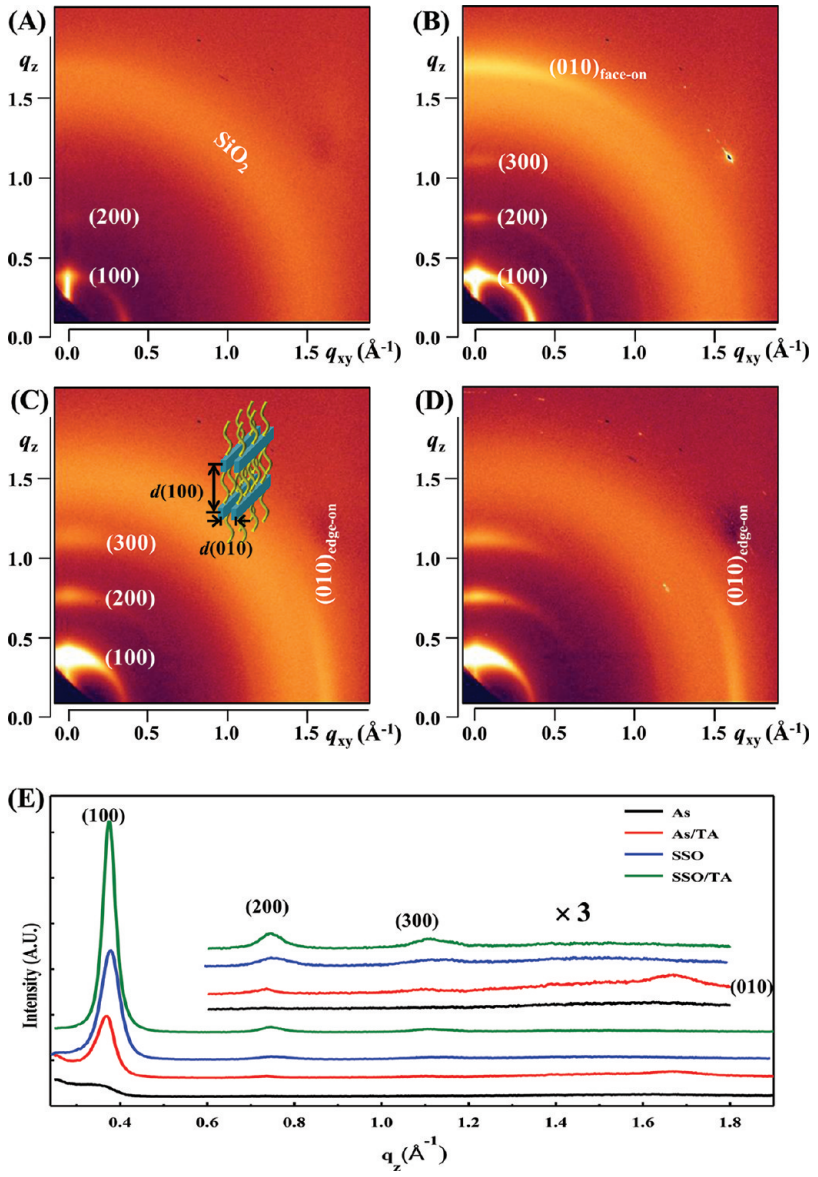

Figure 3. Different orientation and crystallinity of the P3HT domains in the active layers with respect to treatments; 2D-GIXRD patterns of the (A) as-prepared, (B) TA-treated, (C) SSO-treated, and (D) SSO/TA-treated P3HT films, and (E) corresponding 1D profiles of the samples extracted along the out-of-plane axis from the 2D GIXRD patterns. The spray time for SSO was 4 s under an air atmosphere. TA was performed at 135 °C for 30 min under N_2.

pattern developed along the in-plane (q_{xy}) axis, whereas an intense (100) pattern with higher-order spots were observed along the out-of-plane (q_z) axis (Figure 3C). The relatively higher crystallinity of the SSO treated film compared to TA-treated films was demonstrated by the out-of-plane 1D profiles of (Figure 3E), and the (010) peak only being observed in TA treated samples. It is interesting that the chain repacking upon the two post-treatments was considerably different. TA treatment increased the crystallinity of the g-sprayed P3HT films, but a mixture of the edge-on and face-on crystal configuration was displayed in the 2D-GIXRD patterns.[25] In contrast, the 2D-GIXRD patterns of the SSO treated films (Figure 3C)imply that the P3HT chain have a strong edge-on orientation (crystal plane is normal to the substrate), which is preferential for the charge transport.[45] When SSO treated P3HT films were further treated by TA, both the (h00) and (010) plane reflection patterns become more intense without altering their orientation (Figure 3D, E). This result indicates that the TA can crystallize the P3HT chains; however, the effects of this treatment on chain reorientation is limited, whereas the SSO treatment can efficiently rearrange the chain orientation preferentially to the edge-on configuration as well as enhance crystal packing.

Figure 4 schematically describes the P3HT chain configurations in the g-sprayed P3HT active layers upon different post-treatments based on our results. When the active layers are formed by the g-spray method, the P3HT chains are randomly oriented with marginal crystallinity (refer the results in Figure 3A, E) because the fast drying kinetics limit chain ordering.[25,29] Post-TA treatment significantly improved crystallization of the as-sprayed layers through the formation of a polycrystalline complex (mixture of edge-on and face-on configuration) without preferential orientation (Figure 4A, C). These results are in agreement with previous studies, which reported that the crystal orientation cannot be changed by TA at temperatuers below the T_m of the polymers.[33,47] In the case of the post-SSO

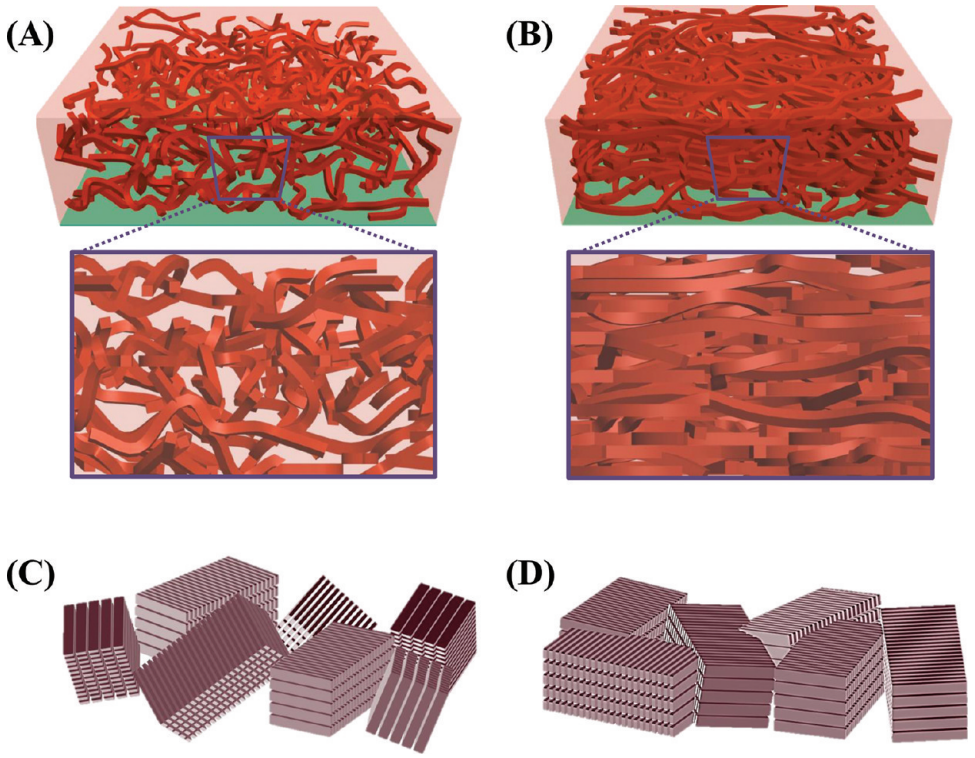

Figure 4. Schematic diagram of the chain packing orientation of the P3HT crystal domains within the active layers. (A, C) The TA-treated active layers contain crystal domains without preferential orientation, whereas (B, D) the SSO-treated active layers contain crystal domains with preferential edge-on orientation. The red wires represent the P3HT crystalline nanofibrils, and the purple bricks represent the chain packed P3HT crystal domains.

treatment, the crystallinity of P3HT was significantly enhanced, and the chains were rearranged dominatly to the edge-on orientation (Figure 4B, D), which was facilitated by the partial dissolving and reassembling of the P3HT by the solvent liquid.[20,48] We have recently shown that SSO can result in the phase segreggation of two organic components in bulk heterojunction structured polymer solar cells (PSC).[20] The efficiency of PSCs was considerably enhanced due to optimizaiton of the nanomorphology of active layers by SSO. The improved OFETs performance using SSO treated active layers was attributed to chain reorientation to the edge-on configuration, which is known to be the preferential ordering for OFETs. The charge transport anisotropy in polymer based FETs, which depends on the chain ordering direction, has been studied by several researchers including Salleo's group.[26,30] The chain orientation direction in P3HT active layers is the most important factor influencing device performance because the packing orientation direction determines the transport rate within the crystals and the types of grain boundaries, which have different intergranular charge transport paths.[26] Charge transport in TA treated P3HT films would be slower due to the higher face-on oriented crystal domain fraction because charge transport through both the face-on domain and at the interface of the face-on/edge-on grain boundaries are much slower than through their edge-on counterparts.[26,45] When SSO treated active layers were subjected to additional TA treatment, the device performance was not significantly enhanced even though the total crystallinity was increased considerably (compare the corresponding 1D-GIXRD profiles in Figure 3E). This fact demonstrates that the chain orientation is the most important factor to device performance and our SSO treatment was a very effective post-treatment method for polymer chain rearrangement.

Similar device performance for spin-coated polymer active films that were post treated with solvent liquid was recently reported by Di et al.[48] In this previous study, the entire process, solvent introduction followed by successive thermal reannealing, took >60 min and the details of the structural changes in the polymer chains were not investigated, although the device performance was successfully enhanced. For our SSO method, the total treatment time takes <5 min at room temperature, and the resulting preferential chain rearrangement to edge-on packing imrpoved the charge mobility by an order of magnitude. It should be also noted that our SSO treatment is an effective chain rearrangement strategy when considered that high molecular weight P3HT (M_n =50 000 g mol^{-1}) was used in this study. It is known that the chain mobility of P3HT reduces dramtically as the molecular weight increases, and it is very difficut to rearrange high molecular weight regioregular P3HT.[9,46,47] SSO was found to be an efficient post-treatment method to facilely control the molecular ordering within active layers, which will be important to high-throughput OFET fabrication techniques.

CONCLUSION

A facile solvent-assisted post-treatment method, SSO, which is adaptable to a spray process, was developed as a practical method to improve the performance of polymer based OFETs. After sprayed P3HT active layers were subjected to SSO treatment, the charge mobility of the devices was enhanced by an order of magnitude as a result of preferential chain rearrangement. Even though the as-sprayed P3HT active layer has a low crystallinity without a particular chain ordering

because of the rapid drying of solvent during film formation, SSO treatment can rearrange the P3HT chains into the preferentially edge-on orientation. On the other hand, TA treatment increased crystallinity without chain reorientation and the face-on and edge-on orientations did not change. The edge-on dominant orientation was the origin of the superior device performance after SSO treatment when compared to TA because charge transport is promoted within edge-on crystal domains, whereas grain boundaries between different crystal orientations (edge-on/face-on) resist charge transport. Our SSO is a simple, room-temperature, external treatment method that can capitalize on the advantages of spray methods for the fabrication of OFETs. We are currently evaluating the effect of SSO in other deposition methods.

■ ASSOCIATED CONTENT

Ⓢ Supporting Information

UV−vis for sprayed P3HT films on the OTS-treated quartz substrates and TEM image and UV−vis spectra of a sprayed P3HT film after TA. This material is available free of charge via the Internet at http://pubs.acs.org.

■ AUTHOR INFORMATION

Corresponding Author

*E-mail: syjang@kookmin.ac.kr.

■ ACKNOWLEDGMENTS

The authors gratefully acknowledge support from the Basic Science Research Program through the National Research Foundation of Korea (NRF), funded by the Ministry of Education, Science, and Technology (2011-0008698), and the Korea Research Council of Fundamental Science & Technology (KRCF) and KIST for 'National Agenda Project (NAP)' program. HCY acknowledges financial support from Basic Science Research Program through the National Research Foundation of Korea (NRF) (2011-0016177). The authors also acknowledge the NSLS at Brookhaven National Laboratory for providing the X9 beamline (DE-AC02-98CH10886).

■ REFERENCES

(1) Gelinck, G. H.; Huitema, H. E. A.; van Veenendaal, E.; Cantatore, E.; Schrijnemakers, L.; van der Putten, J. B. P. H; Geuns, T. C. T.; Beenhakkers, M.; Giesbers, J. B.; Huisman, B.-H.; Meijer, E. J.; Benito, E. M.; Touwslager, F. J.; Marsman, A. W.; van Rens, B. J. E.; de Leeuw, D. M. *Nat. Mater.* **2004**, *3*, 106.

(2) Baude, P. F.; Ender, D. A.; Haase, M. A.; Kelley, T. W.; Muyres, D. V.; Theiss, S. D. *Appl. Phys. Lett.* **2003**, *82*, 3964.

(3) Jung, B. J.; Sun, J.; Lee, T.; Sarjeant, A.; Katz, H. E. *Chem. Mater.* **2008**, *21*, 94.

(4) McCulloch, I.; Heeney, M.; Bailey, C.; Genevicius, K.; MacDonald, I.; Shkunov, M.; Sparrowe, D.; Tierney, S.; Wagner, R.; Zhang, W.; Chabinyc, M. L.; Kline, R. J.; McGehee, M. D.; Toney, M. F. *Nat. Mater.* **2006**, *5*, 328.

(5) Pisula, W.; Tsao, H. N.; Cho, D.; Andreasen, J. W.; Rouhanipour, A.; Breiby, D. W.; Mullen, K. *Adv. Mater.* **2009**, *21*, 209.

(6) Majewski, L. A.; Kingsley, J. W.; Balocco, C.; Song, A. M. *Appl. Phys. Lett.* **2006**, *88*, 222108.

(7) Ong, B. S.; Wu, Y.; Liu, P.; Gardner, S. *Adv. Mater.* **2005**, *17*, 1141.

(8) Huang, T.-H.; Huang, H.-C.; Pei, Z. *Org. Electron.* **2010**, *11*, 618.

(9) Joseph Kline, R.; McGehee, M. D.; Toney, M. F. *Nat. Mater.* **2006**, *5*, 222.

(10) Katz, H. E. *Chem. Mater.* **2004**, *16*, 4748.

(11) Ong, B. S.; Wu, Y.; Liu, P.; Gardner, S. *J. Am. Chem. Soc.* **2004**, *126*, 3378.

(12) Kim, C. H.; Choi, M. H.; Lee, S. H.; Jang, J.; Kirchmeyer, S. *Appl. Phys. Lett.* **2010**, *96*, 123301.

(13) Sirringhaus, H.; Kawase, T.; Friend, R. H.; Shimoda, T.; Inbasekaran, M.; Wu, W.; Woo, E. P. *Science* **2000**, *290*, 2123.

(14) Chan, C. K.; Richter, L. J.; Dinardo, B.; Jaye, C.; Conrad, B. R.; Ro, H. W.; Germack, D. S.; Fischer, D. A.; DeLongchamp, D. M.; Gundlach, D. J. *Appl. Phys. Lett.* **2010**, *96*, 133304.

(15) Bao, Z.; Feng, Y.; Dodabalapur, A.; Raju, V. R.; Lovinger, A. J. *Chem. Mater.* **1997**, *9*, 1299.

(16) Paul, K. E.; Wong, W. S.; Ready, S. E.; Street, R. A. *Appl. Phys. Lett.* **2003**, *83*, 2070.

(17) Lee, K.; Cho, S.; Yuen, J.; Wang, G. M.; Moses, D.; Heeger, A. J.; Surin, M.; Lazzaroni, R. *J. Appl. Phys.* **2006**, *100*.

(18) Moses, D.; Wang, G. M.; Swensen, J.; Heeger, A. J. *J. Appl. Phys.* **2003**, *93*, 6137.

(19) Kim, J.-S.; Chung, W.-S.; Kim, K.; Kim, D. Y.; Paeng, K.-J.; Jo, S. M.; Jang, S.-Y. *Adv. Funct. Mater.* **2010**, *20*, 3402.

(20) Park, H.-Y.; Kim, K.; Kim, D. Y.; Choi, S.-K.; Jo, S. M.; Jang, S.-Y. *J. Mater. Chem.* **2011**, *21*, 4457.

(21) Yamagata, Y.; Ju, J.; Higuchi, T. *Adv. Mater.* **2009**, *21*, 4343.

(22) Saf, R.; Goriup, M.; Steindl, T.; Hamedinger, T. E.; Sandholzer, D.; Hayn, G. *Nat. Mater.* **2004**, *3*, 323.

(23) Tedde, S. F.; Kern, J.; Sterzl, T.; Furst, J.; Lugli, P.; Hayden, O. *Nano Lett.* **2009**, *9*, 980.

(24) Sirringhaus, H.; Bird, M.; Richards, T.; Zhao, N. *Adv. Mater.* **2010**, *22*, 3893.

(25) Yang, H.; LeFevre, S. W.; Ryu, C. Y.; Bao, Z. *Appl. Phys. Lett.* **2007**, *90*, 172116.

(26) Jimison, L. H.; Toney, M. F.; McCulloch, I.; Heeney, M.; Salleo, A. *Adv. Mater.* **2009**, *21*, 1568.

(27) Salleo, A.; Jimison, L. H.; Toney, M. F.; McCulloch, I.; Heeney, M. *Adv. Mater.* **2009**, *21*, 1568.

(28) Salleo, A.; Kline, R. J.; DeLongchamp, D. M.; Chabinyc, M. L. *Adv. Mater.* **2010**, *22*, 3812.

(29) Yang, H.; Shin, T. J.; Yang, L.; Cho, K.; Ryu, C. Y.; Bao, Z. *Adv. Funct. Mater.* **2005**, *15*, 671.

(30) Lee, M. J.; Gupta, D.; Zhao, N.; Heeney, M.; McCulloch, I.; Sirringhaus, H. *Adv. Funct. Mater.* **2011**, *21*, 932.

(31) Chang, J.-F.; Sun, B.; Breiby, D. W.; Nielsen, M. M.; Sölling, T. I.; Giles, M.; McCulloch, I.; Sirringhaus, H. *Chem. Mater.* **2004**, *16*, 4772.

(32) Song, A. M.; Majewski, L. A.; Kingsley, J. W.; Balocco, C. *Appl. Phys. Lett.* **2006**, 88.

(33) Kim, D. H.; Park, Y. D.; Jang, Y.; Yang, H.; Kim, Y. H.; Han, J. I.; Moon, D. G.; Park, S.; Chang, T.; Chang, C.; Joo, M.; Ryu, C. Y.; Cho, K. *Adv. Funct. Mater.* **2005**, *15*, 77.

(34) Sirringhaus, H.; Tessler, N.; Friend, R. H. *Science* **1998**, *280*, 1741.

(35) Kline, R. J.; DeLongchamp, D. M.; Fischer, D. A.; Lin, E. K.; Heeney, M.; McCulloch, I.; Toney, M. F. *Appl. Phys. Lett.* **2007**, *90*, 062117.

(36) Fu, Y.; Lin, C.; Tsai, F.-Y. *Org. Electron.* **2009**, *10*, 883.

(37) Girotto, C.; Moia, D.; Rand, B. P.; Heremans, P. *Adv. Funct. Mater.* **2011**, *21*, 64.

(38) Girotto, C.; Rand, B. P.; Genoe, J.; Heremans, P. *Sol. Energy Mater. Sol. Cells* **2009**, *93*, 454.

(39) Green, R.; Morfa, A.; Ferguson, A. J.; Kopidakis, N.; Rumbles, G.; Shaheen, S. E. *Appl. Phys. Lett.* 2008, *92*.

(40) Zen, A.; Pflaum, J.; Hirschmann, S.; Zhuang, W.; Jaiser, F.; Asawapirom, U.; Rabe, J. P.; Scherf, U.; Neher, D. *Adv. Funct. Mater.* **2004**, *14*, 757.

(41) Moulé, A. J.; Meerholz, K. *Adv. Mater.* **2008**, *20*, 240.

(42) Berson, S.; De Bettignies, R.; Bailly, S.; Guillerez, S. *Adv. Funct. Mater.* **2007**, *17*, 1377.

(43) Zhai, L.; Liu, J. H.; Arif, M.; Zou, J. H.; Khondaker, S. I. *Macromolecules* **2009**, *42*, 9390.

(44) Kline, R. J.; McGehee, M. D.; Kadnikova, E. N.; Liu, J.; Fréchet, J. M. J. *Adv. Mater.* **2003**, *15*, 1519.

(45) Sirringhaus, H.; Brown, P. J.; Friend, R. H.; Nielsen, M. M.; Bechgaard, K.; Langeveld-Voss, B. M. W.; Spiering, A. J. H.; Janssen, R. A. J.; Meijer, E. W.; Herwig, P.; de Leeuw, D. M. *Nature* **1999**, *401*, 685.
(46) McGehee, M. D.; Kline, R. J.; Kadnikova, E. N.; Liu, J. S.; Frechet, J. M. J.; Toney, M. F. *Macromolecules* **2005**, *38*, 3312.
(47) Yang, H.; Joo Shin, T.; Bao, Z.; Ryu, C. Y. *J. Polym. Sci., Part B: Polym. Phys.* **2007**, *45*, 1303.
(48) Di, C. a.; Lu, K.; Zhang, L.; Liu, Y.; Guo, Y.; Sun, X.; Wen, Y.; Yu, G.; Zhu, D. *Adv. Mater.* **2010**, *22*, 1273.